Research Article

On The Determinations of Weather, Seasonal, Sub-Seasonal and Climate Scale Variability and Overall Trends in the Atmosphere and Ocean

LJ Pietrafesa[1,2]*, S Bao[1] and PT Gayes[1]

[1]Coastal Carolina University, College of Coastal Science, P.O. Box 261954, Conway, 5 South Carolina 29528-6054, USA

[2]North Carolina State University, Marine, Earth & Atmospheric Sciences Box 8207, Raleigh, North Carolina 27695, USA

ABSTRACT

The traditional concepts and definitions of multi-scale "weather", "seasonal variability", "sub-seasonal variability", "climate variability", "trends" and "climate change" for both the global atmosphere and the global ocean are considered. We build upon existing literature and present new evidence that atmospheric and oceanic temporal multi-scale variability are the result of a mix of well-known frequency and amplitude modulated nonlinear and phenomena that occur simultaneously [1-3]. We harvest representative atmospheric temperature and wind data, oceanic temperature and coastal water level from United States (U.S.) and United Kingdom (U.K.) agency archives, collected via in-situ and satellite remotely sensed data and employ a mathematical methodology that can decompose nonlinear data. The data decomposition reveals a continuum of well-defined, modulated, internal modes of oscillations, each with broad spectral peaks and each representative of naturally occurring phenomena. We reveal that the conventional notions of weather and seasonal to sub-seasonal to climate variability, actually constitute an over-lapping continuum, with shorter period oscillations commuting with longer period oscillations onto overall record length trends. We relate these internal, intrinsic modes of variability to naturally occurring causal agents, from relatively high frequency weather to lower frequency seasonal to sub-seasonal to climate scale variability. Correlative relationships between climate factors reveal causal couplings of the oceanic and atmospheric systems.

*Corresponding author

LJ Pietrafesa, North Carolina State University, Marine, Earth & Atmospheric Sciences Box 8207, Raleigh, North Carolina 27695, USA. E-mail: len_pietrafesa@ncsu.edu

Introduction

We explore the temporal domains in which the Earth's weather and climate systems reside via the analyses of several revealing environmental data sets that are sufficiently lengthy and complete and which overlap. To pursue that exploration we consider the presently accepted characterizations of "weather" and "climate", per se, in addition to "seasonal", "sub-seasonal" and climate "variability", and climate "trends". Further, we address how these characterizations are determined. The characterizations of these general terms may seem obvious but that is not the case across the spectrum of the broadly defined atmospheric and oceanic communities.

In the AMS "Glossary of Weather and Climate with Related Oceanic & Hydrologic Terms" "weather is the state of the atmosphere, mainly with respect to its effect on life and human activities at a particular time, as defined by the various weather elements and consists of short term, minutes to weeks, variations of the atmosphere [4,5]." There are no oceanic or hydrology definitions of weather in the glossary. The on-line dictionary <http//www.Dictionary.com> states, "weather is the state of the atmosphere at a place and time as regards heat, dryness, sunshine, wind and rain". Again, there are no comparable definitions of the weather of the ocean or of hydrologic weather and the on-line dictionary directs the reader to "climate" when one googles the "weather of the ocean".

Geer defines "climate" as "the total of all statistical weather information that helps to describe the variation of weather at a given place for a specified interval of time" [4,5]. In the AMS Glossary, these definitions of weather and climate apply only to the atmosphere, although on the cover it states, "with related oceanic and hydrologic terms". The on-line <http//www.Dictionary.com> of climate are in keeping with the AMS Glossary. On a seemingly similar tact, with an additional caveat, NOAA's National Center for Environmental Information (NCEI) defines climate in terms of being "the synthesis of weather of some locality, averaged over a span of 30 years, beginning and ending in a calendar year ending in 'zero'. The NCEI synthesis purportedly includes "extremes in weather behavior recorded during that 30 year period or for the period of record." This definition has several contradictory elements in it. For example, a 30-year average of hourly data will not reveal extremes in weather behavior. A "box and whisker" decomposition of 30 years of hourly data would provide this kind

of information, but not a 30-year temporal average [6].

The above definitions seem logical, in that if you average hourly temperatures at a particular location for three consecutive months, then you get the seasonal 3- month average. However, the time series of various state variables may actually have energy in and of itself, at the 3-month period. Therefore, variability in phenomena ranging seconds, minutes, hours, days and weeks, may occupy one broad peak in the energy spectrum and then there may be spectral gaps between two weeks, two months, three months or even six months. Two, three and six monthly phenomena may again be stand-alone, for example, as the Madden-Julian Oscillation propagates and seasons advance and the Earth moves on its axis relative to the Sun, with broad spectral peaks. Annually, oceanic waters sterically rise and drop every three to six months as a function of latitude in response to absorption of the Sun's radiation by the ocean during late Spring to Summer to Fall periods, and then the ocean releases its heat to the atmosphere from late Fall to Winter to Spring [7,8].There is year-to-year variability in the atmosphere and the ocean. Moreover, there are longer period forcing such as multi-year, the 11-year and 22-year Solar Cycles, and the 18.6-year Lunar Nodal and 19-year Metonic Cycles of oceanic astronomical tides [9,10]. Thus, one could argue that while mathematically correct, none of the definitions of weather and climate cited above, and which ignore seasonal to sub-seasonal climate, is physically plausible by extension. Further, there may be a fundamental misunderstanding of what actually constitutes the weather and climate, and of seasonal and sub-seasonal variability therein, of the Earth's atmosphere and ocean. So what of other selected definitions of "weather"?

Orlanski provided an overview of the spatial and temporal scales of atmospheric weather phenomena [11]. Orlanski introduced the concept of a spectral range, which he extended from "micro" or seconds to minutes, "convective" or minutes to tens of minutes, "meso-gamma" from tens of minutes to hours, "meso-beta" from hours to a day, "meso-alpha" from a day to several days, "synoptic" from several days to a week and "planetary" from a week to several weeks. The spatial scales associated with the increasing time scales, also increased. While in Orlanski's view, the phenomena could interact, he speculated that they co-existed independently of each other. No temporal mathematical averaging was necessary in his definitions of "weather".

A view of oceanic short-term to long-term phenomena is in Hill and Rahmstorf [12,13]. Oceanic phenomena range extend in time and space from capillary waves, surface gravity waves, internal waves, the astronomical tides, atmospherically driven phenomena such as fronts, storms and high and low pressure systems, seiches, western boundary currents, planetary waves and the over-turning meridional circulation belt. Oceanic turbulence ranges from the microscale to macroscale to mesoscale, with horizontal scales smaller than millimeters (mms) to larger than 100 kilometers (kms) and vertical scales smaller than mms to larger than 100 meters (ms), with temporal scales of milliseconds to many months. However, at smaller scales, the so-called microscales, these constraints become weak and turbulent motions cross density surfaces. In the upper ocean, microscale turbulence is generated by surface winds, air-sea cooling and evaporation. In the ocean interior, microscale turbulence develops when internal waves develop strong shears and break, much like surface gravity waves.

Regarding the definition of an environmental time series "trend", the Glossary of Weather and Climate is curiously silent, and not mentioned [4,5]. However, Geer does present the definition of a

"normal" as the "average value of a weather element (temperature, precipitation, humidity) over a uniform and relatively long interval covering at least three consecutive 10-year periods, such as those defining the climatological standard normal". This definition is in keeping with the NOAA-NCEI "30-year normal"; in other words a static trend. However, intellectually speaking a 30-year normal does not constitute a trend. Rather, the 30-year normal is a static number, which takes a step, to a new 30-year average, every ten years, beginning and ending with a year ending in zero. Presumably, the tacit assumption is that one connects the 10 year updated average values with a series of lines with differing slopes and this constitutes the NCEI trends in environmental data. As such, it is just a single one computed and updated every new decade ending with a zero, a "static normal".

In our context, we see no physical reason why a "normal" should be a 30-year average and be locked-in as a single, static number produced in consecutive ten-year periods ending in calendar years ending with a 'zero". We believe that the description of the "base modality" of a changing environment, as represented by a state variable, should represent how that variable changes cumulatively over the length of the period being measured, i.e., the entire time series of the variable. Therefore, we recognize the "NOAA normal" as a static number produced as a 30-year average, updated every 10 years on a decade ending with a zero. We hus prefer to introduce the concept of a "dynamic normal". Our "dynamic normal" would be a mathematically tractable and physically meaningful contribution to the definition of a "trend". We define our "dynamic normal" as a moving value that fits a trend curve, of a specific environmental time series including all of the data collected in the total time series. This begs the question, "How do we arrive at such a definition of a trend"? We now review the general literature regarding a "trend".

Several on-line dictionaries, such as <http//www.Dictionary.com> offer definitions such as, "a trend is a general direction in which something is developing or changing" and Wikipedia (www. wikipedia.org/wiki/Linear_regression#Trend_line) which defines a trend as "the long-term linear movement in time series data after other components have been accounted for". Thus, a trend line is drawn through a set of data points, but more properly, their position is calculated using statistical techniques such as linear regression. Wikipedia also states that a trend as "an inclination in a particular direction". While the Wikipedia definition offers more verbiage, the content is essentially the same as that of the on-line Dictionary. The James & James Mathematical Dictionary definition of a trend is: "the general drift, tendency or bent of a set of data" [14]. Chatfiel defines "trend" as "a long term change in the mean" [15]. Nevertheless, difficulties with this latter definition are what "long term" is and what "the mean" is. Further, how can a mean have a trend in it? What if there were variations in climatic variables that exhibit a 50-year cycle. What is the mean of the 50-146 year cycle? If one were to compute 5 year means then the trend would be the line connections of the 10 points; a purely arbitrary choice. Alternatively, if one had only 20 years of data, then the 50-year cycle would appear to be a trend. However, if there were 120 years of data then the 50 cycle would go through two cycles and thus be evident. Therefore, in speaking of a "Chatfield trend" we must take into account the number and span of observations, and then make a subjective assessment as to what constitutes "long term", but also in how one divides a time series into "means" which then create a "trend". Granger insightfully defined a "trend in mean as comprising all frequency components whose wavelength exceeds the length of the observed time series" [16]. However, his definition, which showed

promise in our estimation, was in the context of economics, and thus not recognized by the environmental, geophysical, physical or mathematical sciences. In our opinion, all of the definitions discussed above are not mathematically well-posed excepting for Granger's, which offered real insight.

In a study of sea level variability and trends, Mitchell et al. and Mitchell et al. state that "averaging the water level data over a day, a month or a year forces the astronomical tides to be cancelled out, leaving behind climate signals". Actually, left behind from such an averaging process is a confused data set. In the words of Silver, "you have reduced the signal to the noise" [17]. Likewise, averaging weather data is not a recommended approach to de-convolving the data in an attempt to reveal the internal, intrinsic variability buried within a time series of water level data. In addition, given the above discussion of how you actually define a trend and what the process of de-trending a time series actually entails, one cannot easily determine an actual "rate" of sea level rise or fall. Prior studies have computed so-called trends of water level rise (or falls) using conventional averaging techniques that generally lead to a straight line or a series of connected straight-line segments. However, in doing so, how is the span of time employed in the averaging process determined? Here, if a time series shows no change in the mean, then broadly speaking the time series would be "stationary". Clearly the fact that sea level time series have non-zero slopes over record lengths suggests that the times series are by intrinsic constitution, "non-stationary" and "nonlinear". The same fundamental principles that apply to coastal sea level data, also apply to atmospheric state variable data. If you visually interrogate all atmospheric and oceanic temperature and water level data sets, and wind time series, there is a cross cutting strong sense of both non-stationary and nonlinear temporal variations within the time series. As such, it is not clear that any conventional simple averaging process can reflect what information is buried in the time series. Therefore, the question arises, "is there a mathematically rigorous process that will allow a "trend", yet to be defined, to be calculated?

Wu et al. presented a logical mathematical approach to the definition of "a trend" that is appropriate for any continuous time series, including those that are non-stationary and nonlinear [18,19]. In that work, a trend devolves as an empirically determined function within the temporal span of a data set, in which there can be at most one extremum. Being intrinsic, the method to derive a trend has to be adaptive; that is, it must fit the span of the data. Thus, the definition of trend in this publication presumes that a time scale exists, dictated by the temporal span of the data, thus a logical and mathematically based definition suggested previously by Granger [16]. All the above requirements suggested to Wu et al. that the Empirical Modal Decomposition (EMD) method first presented by Huang et al. As the logical choice for an algorithm that could determine the trend in any continuous data set [18-20]. Huang et al. employed a Hilbert Transform to decompose continuous time series. Moreover, in the process of determining the trend of a data time series, internal mode functions (IMFs) of variability buried within the time series are revealed [21,22]. We will pursue this approach. We also note that Flandrin et al found occasional cross talk between consecutive IMFs [23]. To address this, Wu and Huang introduced white noise into the Hilbert Transform (HT) and EMD process decomposition, thereby eliminating the cross talk and effecting the "Ensemble" EMD or EEMD [19]. The 198 'gravest' intrinsic mode or the lengthiest mode of a time series was then determined by employing the EEMD methodology, so that there is but one respective extremum, either a maximum or a minimum, in this mode, even though this mode can go up or down

or up and down or down and up, in amplitude. They called this "gravest mode" the "trend" of the time series. With this definition of trend, the variability of the data over intrinsic time scales is calculated. We next employ the EEMD method, as presented by Wu and Huang to decompose a small set of relatively lengthy state variable time series and well-known planetary climate factors, to determine if actual data can help us better understand the concepts of weather, seasonal to sub-seasonal variability, climate variability, and trends, and several relationships therein [19]. It is of note that Bothe [24] posed the question "when does weather become climate". We will answer that question.

Data
Data used in our study are representative of atmospheric and oceanic state variables covering the suite and spectrum extending across high to low frequency phenomena in both the atmosphere and the ocean. These data include hourly air temperature, atmospheric wind and coastal water level time series from Charleston, South Carolina (SC) and air temperature data from Fairbanks Alaska (AK) and oceanic sea surface temperatures collected via a series of National Oceanic & Atmospheric Administration (NOAA) GOES satellites. These data are especially key to establishing the climate factors utilized in this study. The reasons that the AK and SC data were selected in this study is that the time series are continuous and complete, so that no breaks in the time series occurred so no artificial data were introduced. Additionally, while many other stations could have been studied, and in fact were, we reduced the number to a minimum as the data decompositions all showed the same results. Moreover the AK and SC stations are as distant from one another as you can get in the U.S.

Higher frequency atmospheric and oceanic data, such as hourly samples, are routine in the atmosphere with temperature, pressure and other state variable data monitored across the U.S. since 1895, and even earlier, and of coastal sea level. This is not the same for oceanic time series, with coastal water level data being the most consistent and lengthy. In addition to land based atmospheric data and coastal ocean water level data, we also harvested monthly Solar Sun Spot, several well-known climate factor data from the North Atlantic and Pacific Ocean Basins, Global Surface Temperature Anomaly (GSTA), Western Boundary Current (WBC), Oceanic Heat and a 17th Century temperature time series from Central England (CE). Collectively the data were obtained from NOAA NCEI archives, http://www.ncei.noaa.gov/ the Climatic Research Unit, UK Meteorology Office, Hadley Centre, http://www.cru.uea.ac.uk/cru/info/,http://www.cgd.ucar.edu/cas/jhurrell/naointro/, html.http://www.esrl.noaa;http://jisao.washingtonedu/do/PDO.latest, ftp://www.coaps.fsu.edu/pub/JMASSTIndex/.

We also investigate several time series of climate scale phenomena which we obtained from the three sites listed above. We consider the time series of Central England (CE), Solar Sun Spot activity, the Global Land Surface Temperature Anomaly Time Series (GLSTA), Oceanic Heat, the El Niño Southern Oscillation (ENSO), the Atlantic Multi-Decadal Oscillation (AMO), the Pacific Decadal Oscillation, the Artic Oscillation (AO) and the North Atlantic Oscillation (NAO). Monthly data sets are analyzed, as those are available from the NCEI website and cover comparable periods to the CE time series. The NAO is the normalized pressure difference between the Azores and Reykjavik, Iceland. ENSO is a temporal scale fluctuation in sea surface temperature and air pressure in the equatorial Pacific Ocean. The AO is an atmospheric circulation pattern in which the atmospheric pressure over the Arctic polar region varies in opposition with that over middle latitudes [25].

The NAO and the AO are different ways of describing the same phenomenon so the AO decomposition is not shown [25]. The PDO is the leading principal component of North Pacific monthly SST variability, poleward of 20°N. Purportedly, ENSO and the PDO have similar spatial climate fingerprints, but very different behaviors in time. The Atlantic Multi-decadal Oscillation (AMO) is the mean SST between 75˚W and 7.5˚W and south of 60˚N. We also consider two very old coastal water level records from San Francisco CA and Delfzig, the Netherlands.

Results and Discussion
In Figure 1, the Air Temperature time series and EEMD IMFs for Charleston (Top of the Panel is the hourly time series) ranging from 0 to 40 °C. In the 73-year hourly time series, we find 18 Oscillatory EEMD IMF modes and the 19th mode, the overall gravest mode, is the trend. The modes are stacked top to bottom in order of increasing period (and the range in temperatures in °C). Mode 1 is 2-3 hourly (+/-3 °C) Mode 2 is 6-hourly (+/- 5 °C), Mode 3 is 12 hourly (+/- 10 °C) and Mode 4 is 24 hourly (+/-10 °C). Mode 5 is 2-4 days (+/-8 °C), Mode 6 is 5-10 days (+/-8 °C), Mode 7 is 1-2 monthly (+/- 8°C), Mode 8 is 3 monthly (+/- 8 °C) and Mode 9 is ~ 6 monthly (+/- 3 °C). Mode 10 is yearly (+/- 15 °C). Mode 11 is 2-3 years (+/-8 °C), Mode 12 is 3-5 years (+/- 2 °C), and Mode 13 is 5-7 years (+/-2 °C). Mode 14 is 10-12 years (+/- 2 °C), Mode 15 is ~ 20-22 years (+/- 2 °C), IMF 16 is 32-34 years (+/- 0.5 °C), IMF 17 is ~ 65-70 years (+/- 0.5 °C), and Mode 18 is ~ 120-140 years (+/- 0.5 °C), as the first half of a 140 year oscillation. Mode 19 is the 73-year record length trend and shows a 2°C rise at the site.
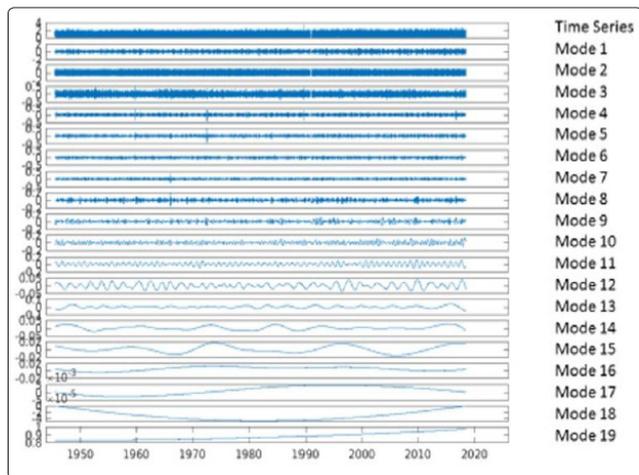

Figure 1: The Air Temperature time series and EEMD IMFs for Charleston (Top of the Panel is the hourly time series) ranging from 0 to 40°C. In the 73-year hourly time series, we find 18 Oscillatory EEMD IMF modes and the 19th mode, the overall gravest mode, is the trend.

In Figure 2, we see the water level hourly time series and EEMD IMFs for Charleston SC (Top of the Panel is the 73 year hourly time series) ranging from 0 meters (m) to 4 m. It is of note that the tidal range at Charleston is generally less than 2.5 m but one event in 1990 upped the overall range record and we chose not to clip the data point. There are 18 oscillatory EEMD IMF modes and the 19th gravest mode, the trend. The modes are stacked top to bottom in order of increasing period (and the range in amplitudes). Mode 1 is 3-6 hourly, higher harmonics of the M2 Tide (+/-1.0m). Mode 2 is

the Semi-Diurnal M2 12.42 hourly Tide (+/-2.0m), Mode 3 is the inertial signal at ~ 18 hours (+/-0.5m) and Mode 4 is the Diurnal S2 or 24 hourly (+/-0.5m). Modes 5 and 6 are atmospheric wind driven 2-4 day (+/-0.5m) and 5-7 day (+/-0.5m), signatures respectively. Mode 7 is 14 days or the fortnightly (+/-0.5m) tide. Mode 8 is 3-monthly (+/-0.2m) and Mode 9 is 6-monthly (+/-0.2m). Mode 10 is annual (+/-0.2m). Mode 11 is 2-3 years (+/-0.2m), Mode 12 is 3-5 years (+/-0.05m), and Mode 13 is 5- 7 years (+/-0.05m). Mode 14 is 11 years (+/-0.05m), Mode 15 is 22 years (+/-0.02m), 16 is 33 years (+/-0.00002m), 17 is 70 years (+/-0.00005m), and 18 is the first half cycle of a 140 year mode (+/-0.00004m). Mode 19 is the 73-year (record length) trend and shows a water level rise of 0.027 m or 0.365 cm/yr. We note that IMF 10 is the "annual" mode and is relatively stable with +/- amplitudes of less than 15 cm. However, in the annually averaged plot (Figure 3a) there is a large jump of 25 cm, which occurs in the 1940's –1950. The question is, where is this jump reflected in Figure 4? The answer is, in the lower frequency, IMFs of 13–18, all of which are in a quasi-decade long upward swing in amplitude.
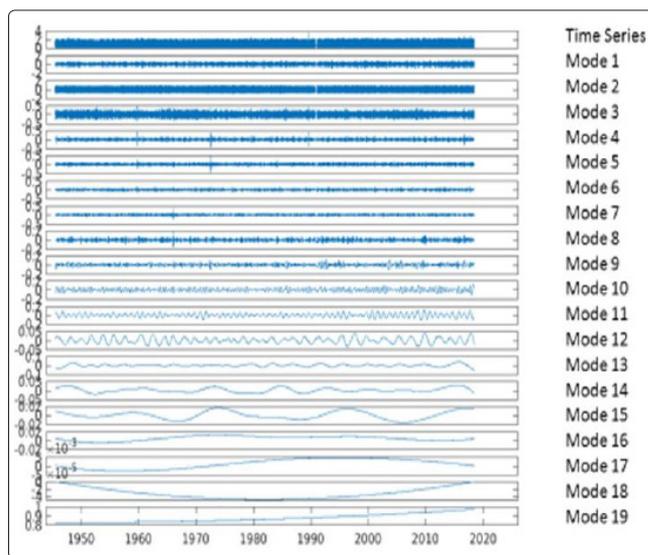

Figure 2: Hourly Water Level data at Charleston SC dating from 07/01/1945 through 06/30/2018. The original time series is in the top panel. There are 19 EEMD IMF modes presented from Top to bottom, in increasing period where IMF 19 is the overall record length trend. Units are in Meters.

The Hilbert Energy Spectra (not shown because it requires multiple individual figures as a function of frequency bands) clearly reveal a spectra continuum with distinct highs and lows at periods shorter the very strong signals at 365 days (0.15X10⁻⁵Hz) and at 24 hours (1.157X10⁻⁵Hz). Between a day and a year are equally robust signals with periods of 2-10 days, and 2, 3 and 6 months. This documents a continuum of high frequency short period atmospheric variations to lower frequency, longer period variability with distinct temporal peaks. One could interpret these continua in highlighted bands running through consecutive years as "weather" to "seasonal to sub-seasonal" to "annual" variability. There are a series of well-defined spectral peaks at 2-4, 5-7, 11, 22, 33, 70 and 140 years. While the IMFs and the Hilbert (HES) spectra indicate changes in amplitude and intensity, representative examples of how averages over any time scales can vary are in Figure 3.
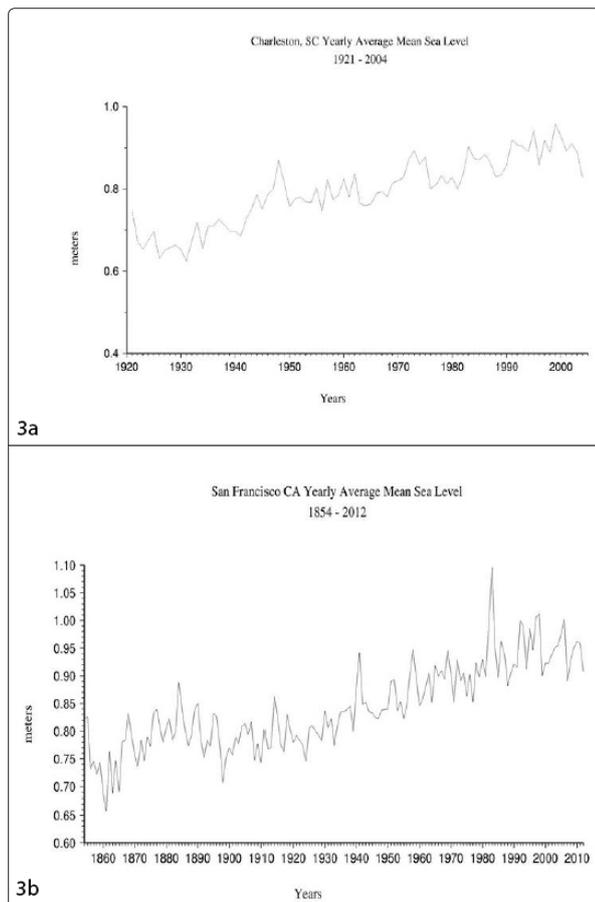
3a

3b

Figure 3: Yearly averaged hourly time series of: a. Charleston SC; b. San Francisco CA

Figures 3a and 3b, present the time series of yearly average hourly water levels for Charleston SC and San Francisco CA. These two stations are selected as they are on opposite sides of the U.S. and because both have continuously complete, hourly time series. As can be seen, one to two year differences of up to 25 cm for the overall annual averages of water level are evident. During the 1920s and into the mid-1930s there were relative lows in both the Pacific and Atlantic Ocean basin water level time series as shown in Figures 3a and 3b. The San Francisco time series indicates that the relative drop started in the mid-1880s. The time series then display a 15-year period of rapid rise from the mid-1930s to 1950, followed by a gradual rise up to the present, with a minor slowing over the past decade. These decadal to multi-decadal relative drops and rises in the time series are characterized by high amplitude, +/- 5 to 20 cm, 1 to 2-year variations. Recall that a yearly average, by definition contains all of the internal IMFs of variability for that particular year. We will next consider the EEMD decomposition of the Charleston water level hourly time series and reveal the differences between a "yearly average" and an "annual" signal.

We next consider a 70-year hourly temperature data set, from Fairbanks AK and subject it to EEMD decomposition (Figure 4a). Here we find 18 IMFs of temporal variability; including the trend as the 18th mode. We find that within the decomposition the internal modes represent: 3-6 hourly; 12 hourly; 24 hourly or diurnal; 2-4 days; 6-8 days; 1-2 monthly; 3 monthly; 6 monthly; annual; 2-3 years; 5-7 years; 11 years; 22 years; 33 years; and ~ 65-70 years; for a total of 17 modes in the nearly 69 year time series. The 18th mode is the red line in the upper panel. Modes

9–17 are presented in Figure 4. Using definitions cited in the text above, internal modes 1–6 would be termed "weather" while those from 7–11 would be "seasonal" to "sub-seasonal" variability in frequency, and 12 through 17 would be "climate" variability. Collectively the 17 oscillating modes constitute a temporally modulated continuum of air temperature variability which ranges from very high frequency- short period "weather" to seasonal to sub-seasonal to annual to inter-annual to decadal to multi –decadal, and thus to climate scale variability. In Figure 4, we also see modes 7-11 of the Charleston hourly data sets superimposed on the Fairbanks AK time series. The overlays are remarkably alike, save for Mode C8 from the Charleston data set vs. the Mode 17 from Fairbanks data set, which is 180° out of phase. Recall that Charleston is at latitude of ~ 32.8°N along the southeast coast of the U.S. while Fairbanks is at ~ 64.8° N in the far reaches of the northwest U.S. This could reflect a flip of the 70-year mode in the northern part of the Pacific Ocean Basin (POB) versus the southern part of the North Atlantic Ocean Basin (NAOB). Missing from the Fairbanks temperature time series is the 140-year mode. Why, because the time series is a year or two too short to capture the first 70 year half of the 140- year oscillation. Another question, which Figure 4 vs. Figure 1 addresses, is that a temporal averaging, in this case monthly of the hourly data, of the time series of air temperatures at Charleston does not change the lower frequency IMF mode distributions which occur over much longer periods of variability and thus are not affected by the mathematical monthly averaging process. This is not the case for hourly vs monthly Charleston coastal sea level data, as we show later in the text.
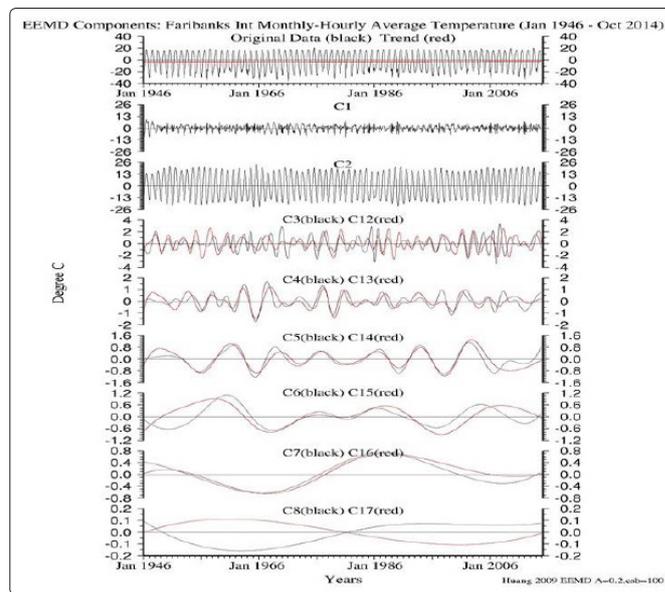

Figure 4: EEMD decomposition of the Fairbanks AK hourly atmospheric temperature data collected from 01/1946 -11/2014, modes 9-17 (note Modes 1-8 are not shown as they are identical to those from Charleston SC in Figure 1); b. the EEMD decomposition of monthly averaged data from 01/1946-11/2014 at the NWS stations in Fairbanks AK (--line) and Charleston SC (--line)

In Figure 5a we present the EEMD of the alongshore wind component time series at Charleston. There are 19 modes. Modes 1-8 are identical to the atmospheric temperature modes shown in Figure 1, so not shown. There are 18 Oscillatory EEMD IMF modes and the 19th mode, the gravest mode, the trend. The modes are stacked top to bottom in order of increasing period (and the range in temperatures in °C). Mode 1 is inter-hourly (+/-3) Mode 2 is 6-hourly (+/- 5), Mode 3 is 12 hourly (+/- 10) and Mode 4 is

24 hourly (+/-10). Mode 5 is 2-4 days (+/-8), Mode 6 is 5-7 days (+/-8), and Mode 7 is 1-2 monthly (+/- 8). Mode 8 is 3 monthly (+/- 8) and Mode 9 is 6 monthly (+/- 3). Mode 10 is annual (+/- 15). Mode 11 is 2-3 years (+/-8), Mode 12 is 3-5 years (+/- 2), and Mode 13 is 5-7 years (+/-2). Mode 14 is 11 years (+/- 2), Mode 15 is 22 years (+/- 2), 16 is 33 years (+/- 0.5), 17 is 65-70 years (+/-0.5), and Mode 18 is 140 years (+/- 0.5), as the first half of a 140 year oscillation is evident. Mode 19 is the 73-year record length trend and shows about a 2°C rise at the site.
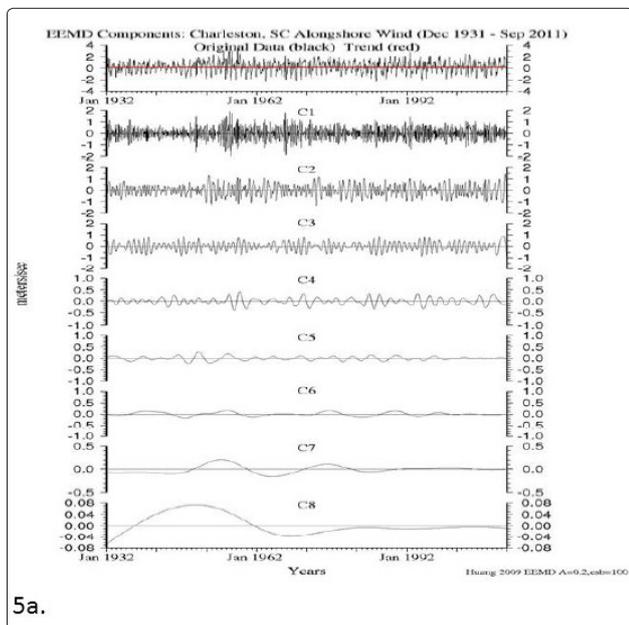
5a.
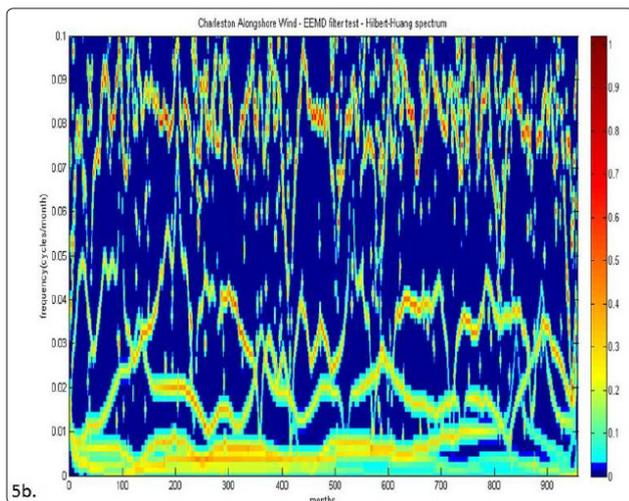
5b.

Figure 5: a. EEMD of the hourly alongshore wind component at Charleston SC from 12/01/1931-09/30/2011 (the first 8 high frequency modes are not shown as they are identical to Modes 1-8 in Figure 1); b. HES Spectrum of the Charleston Alongshore Wind Time Series presented in the upper panel of (a).

The HES shown in Figure 5b displays rich energetic spectra as a function of frequency persisting throughout the entire time series. As first presented by Pietrafesa, an FFT of the same time series would show a spectrum with several high frequency bumps below 5- 7 days, and then a slow rise into a flat spectrum to lower frequencies (< 0.1cpd); not very revealing. FFTs cannot display nonlinear, non-periodic phenomena in any detail [8]. Alternatively, in the HES, which deals with nonlinear, non-periodic data, we see high to low frequencies at varying energy intensities throughout the entire 80-year time series. The HES energy spectrum suggests

there are low to high period phenomena represented at all times, co-existing, across the entire time series, a manifestation of a suite of phenomena with differing time scales.

We next revisit the EEMD of the Charleston SC hourly water level time series, from 1921–2007 (Figure 2). With the hourly time series, we found that there are 17 variable modes and a trend. Curiously, in this data set, the Metonic Cycle appears to be missing. The Metonic Cycle is a period of 19 years that is remarkable for being an integer multiple of the solar year and the synodic (lunar) month. The Greek Astronomer Meton of Athens (5th Century BC) observed that a period of 19 years is exactly equal to 235 synodic months and 6,940 days. The difference between the two periods (of 19 years and 235 synodic months) is a few hours, truly remarkable given the definition of a day and a year. This is bothersome that the 19-year cycle appears to be absent. However, a closer look at IMF 1 shows modulations, exactly 19 years long, with amplitudes of +/- 2 cm; an important finding. Figure 6 has implications or sampling periods of any continuous time series and indicates that if you do not have a high enough sampling frequency, you could miss very long period, i.e. decadal to multi-decadal period, oscillations. It also says that coastal water level data contains truly deterministic components; the astronomical tides. These are the only deterministic phenomena in the global ocean. The spikes shown in the time series presented in Figure 7 are due to atmospheric wind driven water level events, which can reach amplitudes of +/- 90 cm. the atmospheric wind field, a stochastic forcing function, is causal and is a strong driver of coastal sea level along all coastlines of all continents globally.
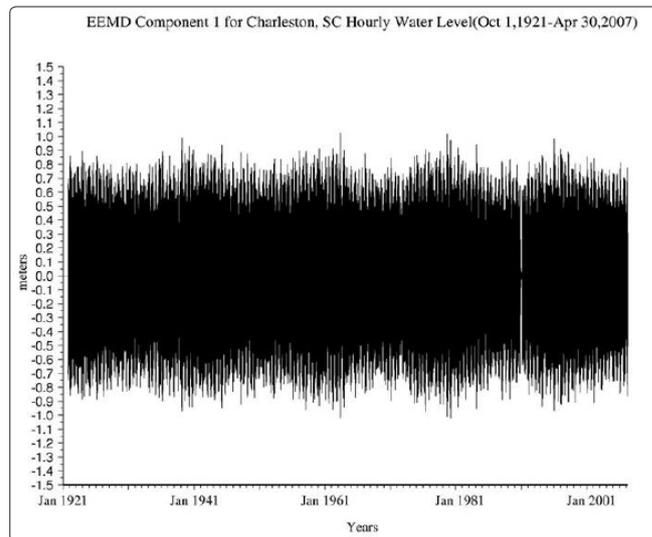

Figure 6: EEMD IMF 1 of the Charleston SC hourly coastal water level data time series, dating back to 1921, showing the 19-year modulation of the decomposition. (Note the missing data point).

The question then arises: Are there naturally occurring phenomena which display these 19 internal, intrinsic modes of variability? To review, at the high frequency end of the spectrum, in the atmospheric, the hourly data, from shorter periods of hours to days, should reveal the presence of thermals, fronts, squalls, thunderstorms, diurnal variability, mesoscale events, high and low pressure systems, mid-latitude cyclones, tropical cyclones extending to planetary waves, the order of a month, the Madden-Julian Oscillation of ~ 2 months and then on to 3 and 6 month seasons. Similarly in the ocean, there are hourly internal waves, water spouts, higher harmonics of the astronomical tides, tsunamis, the Semi-Diurnal Lunar M_2 tide, inertial motions, the Diurnal Solar S_2 tide, several day atmospheric wind driven events

listed previously, fronts, 2-12 day Western Boundary Current frontal waves, multi-day to several weeks to monthly mesoscale eddies, and seasonal steric rises and falls [8]. In the atmospheric temperature and wind time series, and in the coastal sea level time series, weather phenomena have collectively made their presence known in IMFs 1, 2, 3, 4, 5, 6, and 7 while Modes 8, 9 and 10 are seasonal to sub-seasonal to Mode 11, which is annual, and Mode 12 is the U.S. Senate Bill 1331 extent of the sub-seasonal definition of 2 years. For Modes 13 – 18, we will investigate some common sub-seasonal to multi-yearly to multi- decadal to centennial scale signatures, which occur at climate scales.

The monthly data time series and EEMD IMFs of CE, Solar activity, the GSTA and ENSO, are shown in Figures 7 a - d. In Figure 7a, we consider a time series, collected in a region of Central England (CE), dating back to 1659. To our knowledge, this is the Earth's oldest land based, continuous temperature time series, available from the Hadley Center. The CE time series and its EEMD modal decomposition are in Figure 9 (upper left). IMFs of 3 and 6 months, 1-2, 4-7, 11 (the Schwabe Cycle), 22 (the Hale Cycle), 33, 65 and 140 years. Solar Sun Spot activity, a potential causal agent, displays IMFs of 3 and 6 months, annual, 4-7, 11, 22, 65 and 140-year activity; with Modes 3,4,5 all modulated by11 year burst packets. ENSO IMFs 1 -7 of the four separate time series are uniform and reflect periods of 3 and 6 months, 1-2, 5-7, 11, 22, 33, 65, and 140 years, respectively. The GLSTA (and GOSTA and GSTA, not shown) display the same cycles as ENSO. The "trends of each time series are shown as red lines.
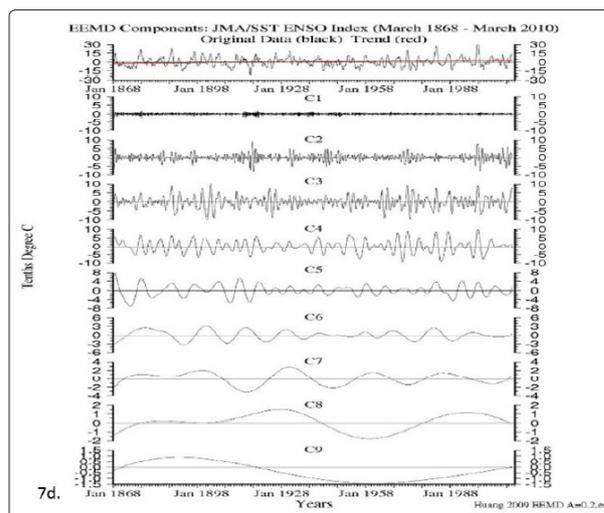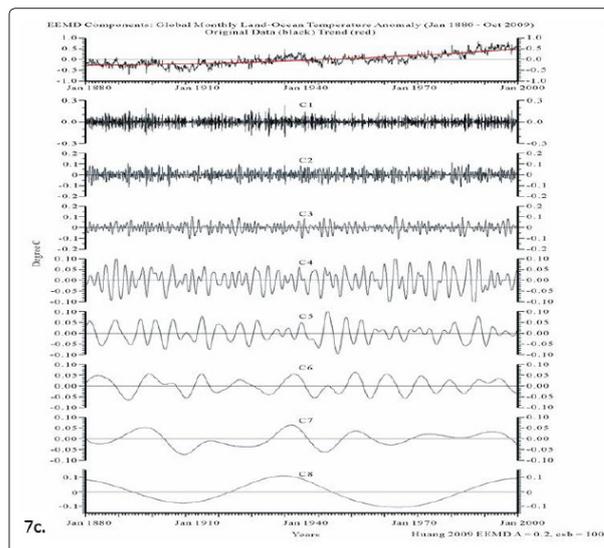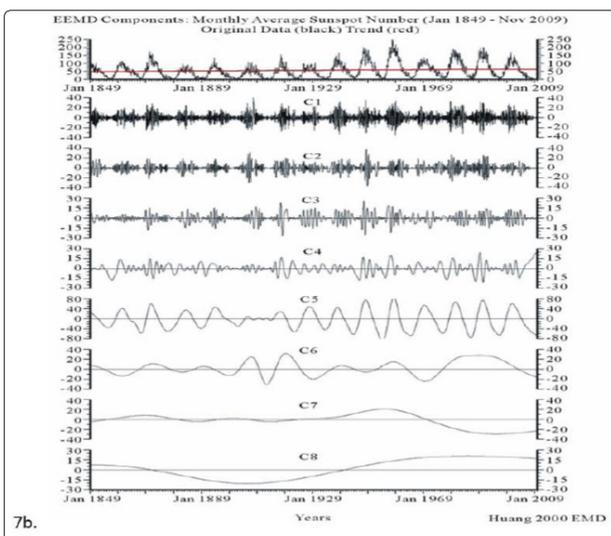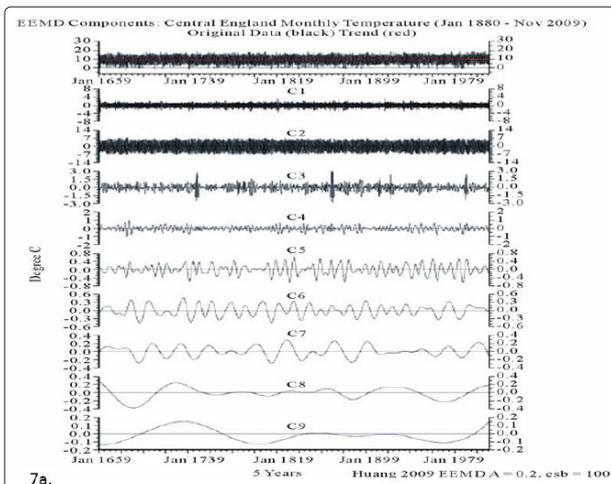
7a.

7b.

7c.

7d.

Figure 7: EEMD IMFs of: a. the 350 year time series of monthly temperatures in Central England (CE); b. Monthly Solar Sun-Spot activity; c. the GLSTA monthly time series; d. the ENSO monthly time series.

In Figure 8 a – c, we present the EEMD IMFs of the monthly time series of the "unsmoothed" version of the AMO, the NAO and the PDO. Each climate factor displays the same number and monthly to annual to yearly variability in their intrinsic modes as do those of the GLSTA (also the GOSTA and GSTA, not shown). We do not show the Quasi-Bienniel Oscillation nor the Atlantic Meridional Mode as they do not add information to the decompositions shown. The PDO is a shorter time series so does not contain the 140-year cycle shown in the ENSO decomposition. The NAO and by association, the AO (not shown) mimic the Solar decomposition, as well. The Earth's atmospheric and oceanic climate variability are related to the redistribution of Solar Radiation (read "heat") in temperature and pressure on the planet. The sub-seasonal to climate variability of well-known climate factors shows up in land and sea temperatures, atmospheric winds and sea level variability.
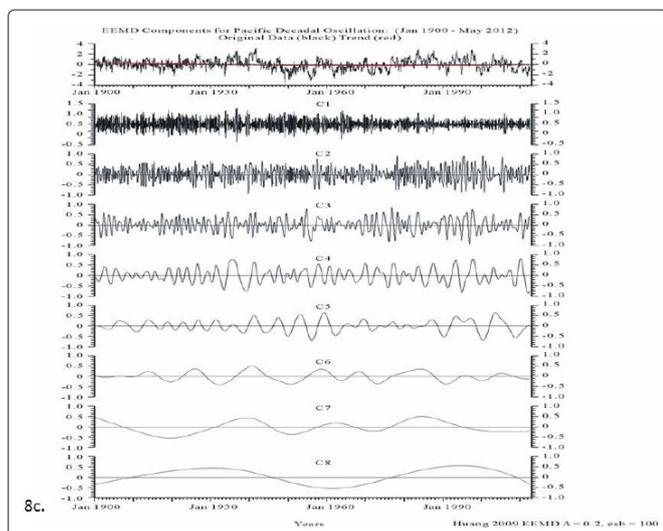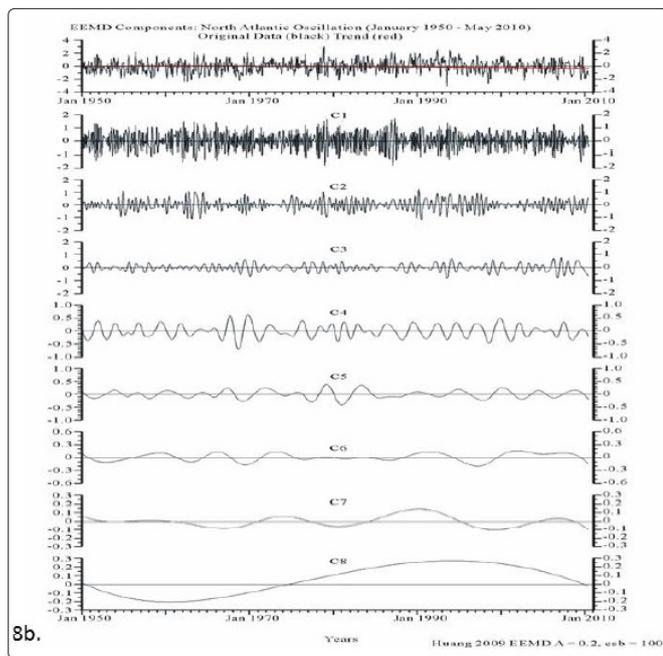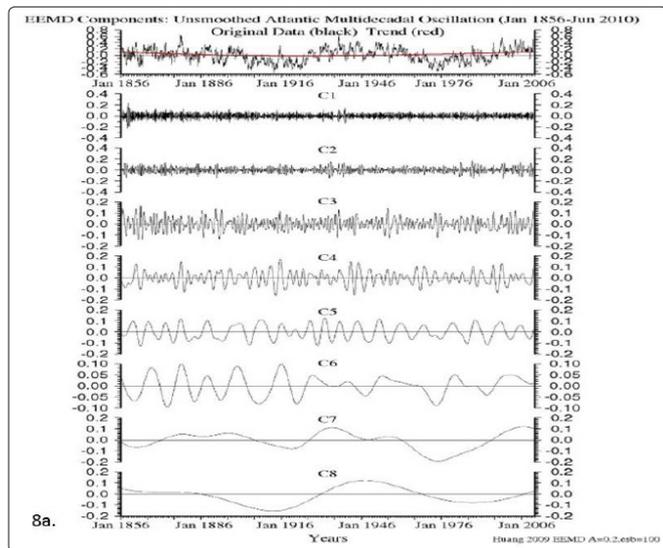
8a.

8b.

8c.

Figure 8: a. the AMO; b. the NAO; c. the PDO.

In Figures 9 a and b we present the EEMD IMFs of monthly water level of San Francisco CA and Delfzig, the Netherlands, both dating back to the mid-19th Century (1854 for the former, 1865 for the latter). Both locales are on the eastern sides of oceanic water basins, San Francisco in the northern Pacific and Delfzig in the northern Atlantic. Remarkably, there are 9 IMFs in both monthly time series: C1 and C2 are 3 and 6 monthly, respectively, C3 is 1 4 year, C4, C5, C6, C7 and C8 are 2-4, 5-7, 11, 22 and 65-70 years, respectively. Modes C8 and C7 are curiously 180o out of phase with each other. In the San Francisco and Delfzig IMFs, we find the 33-year mode.
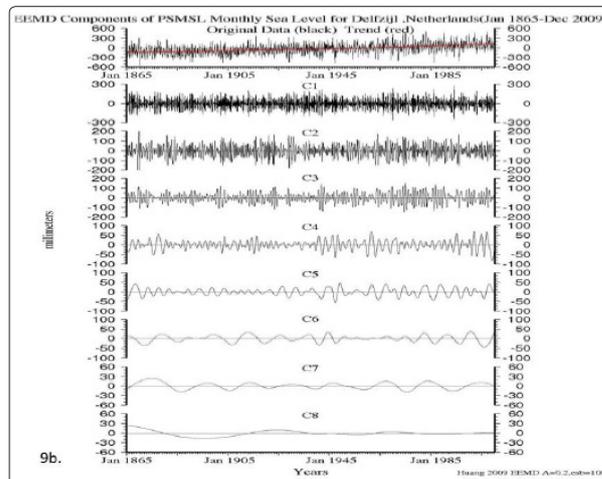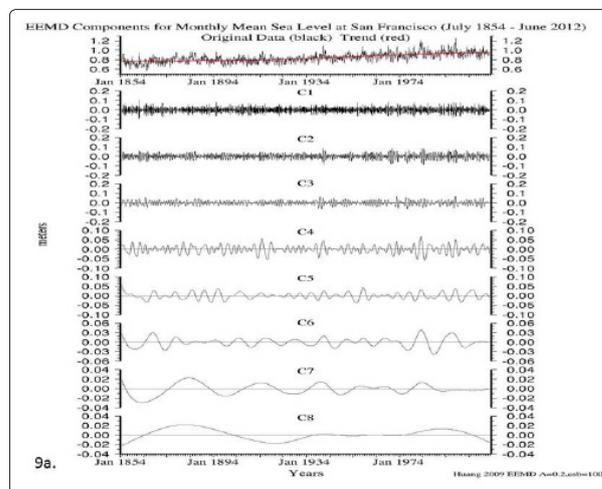

9a.

9b.

Figure 9: EEMD IMFs of Sea level time series from: a. San Francisco CA; b. Delfzig, the Netherlands.

In Table 1, we present the EEMD IMF decomposition of the weather and climate state variables and several of the well-known planetary drivers. IMFs are the Intrinsic Mode Functions. Period is the temporal central IMF signal. Time series of Atmospheric Temperatures (ATs), Coastal Sea Levels (CSLs) and Coastal Alongshore Winds (CAWs) are collected hourly. Central England atmospheric temperatures (CE), Solar activity (SUN), the El Nino Southern Oscillation (ENSO), the Pacific Decadal Oscillation (PDO), the North Atlantic Oscillation (NAO), the Artic Oscillation (AO), the Atlantic Meridional Oscillation (AMO), the Global Land Surface Temperature (GLSTA), the Global Ocean Surface Temperature (GOSTA), the Global Surface Temperature (GSTA) and the Western Boundary Current (WBC) time series, are all monthly averaged data time series. The Ocean Heat Content (OHC) time series is 3-monthly. Table 1 shows that there is ordered and consistent structure in the temporal variability of weather and climate time series of state atmospheric and oceanic variables.

The hourly time series data sets all display 18 IMF modes of variability. The 19th modes are "trends". As a function of length of the time series, the atmospheric and oceanic monthly time series display up to 11 IMFs, with a 12th, the trend, and the one 3-monthly time series (OHC) containing only 6 IMFs and a 7th, the trend.

Table 1

a.IMFs#→	1	2	3	4	5	6	7	8	9	10	11	12	13	14	15	16	17	18
b.IMs #→								1	2	3	4	5	6	7	8	9	10	11
Period→	hr	hr	hr	hr	dy	dy	mo	mo	mo	mo	y	y	y	y	y	y	y	y
Series ↓																		
ATs	2-3	6	12	24	2-4	5-8	1-2	3	6	12	2-3	3-5	5-7	11	22	33	65-70	120-140
CE								3	6	12	2-3	3-5	5-7	11	22	33	65	140
CSLs	3-6	12.42	18	24	2-4	5-8	0.5	3	6	12	2-3	3-5	5-7	11	22	33	65-70	120-140
CAWs	2-3	6	12	24	2-4	5-8	1-2	3	6	12	2-3	3-5	5-7	11	22	33	65-70	120-140
SUN								3	6	12	4-7	11	22	33	65-70	140		
ENSO								3	6	12	4-7	11	22	33	65-70	140		
AMO								3	6	12	4-7	11	22	33	65-70	140		
NAO								3	6	12	4-7	11	22	33	65-70	140		
AO								3	6	12	4-7	11	22	33	65-70	140		
PDO								3	6	12	4-7	11	22	33	65-70	140		
GLSTA								3	6	12	4-7	11	22	33	65-70	140		
GOSTA								3	6	12	4-7	11	22	33	65-70	140		
GSTA								3	6	12	4-7	11	22	33	65-70	140		
WBC								3	6	12	4-7	11	22	33	65-70			
OHC									6	12	4-7	11	22	33				

We next consider the relationships between the climate factors that we have considered in Table 1. In Table 2 we present cross-correlations between the IMFs of the GSTA and climate factors. In Table 3 we present the cross-correlations of the IMFs of the CE and climate factors.

Table 2: Cross-correlations between the GSTA (Monthly Ocean + Land surface temperature anomaly IMFs and climate factor IMFs.

	AMM	AMO	AO	JMA	NAO	PDO	QBO	SUN
Original	0.121	0.4345	0.1648	0.3479	0.0524	0.0915	0.0424	-0.0486
Mode 1	0.0386	−0.0675	0.2129	0.079	0.0196	-0.05430	0.0397	0.0333
Mode 2	−0.0703	0.108	0.2221	0.1415	0.1169	0.0658	0.0872	-0.0642
Mode 3	−0.1304	0.202	0.1739	0.3107	0.0341	0.0093	0.0861	0.0927
Mode 4	0.1321	0.7088	-0.1828	0.574	-0.0137	-0.005	-0.0111	-0.0604
Mode 5	0.3058	0.5533	-0.1606	0.6056	-0.2423	-0.1692	0.1389	0.1595
Mode 6	0.3144	0.2792	-0.1284	0.2921	-0.0809	-0.3103	0.005	0.1463
Mode 7	-0.23870	0.2227	-0.5282	0.2976	-0.171	0.3724	0.0353	0.1086
Mode 8	0.2423	0.1401	0.5863	0.5528	0.3958	0.215	-0.163	-0.8641
Trend	0.5202	0.9982	0.305	0.9999	-0.938	0.7615	0.6548	-0.7213

If $|r| \geq 0.074$ correlation is considered to be statistically significant ($p < 0.05$, color = red); If $|r| \geq 0.130$ correlation is considered to be extremely statistically significant ($p < 0.001$, color = pink). Number of Samples: N = 718 (Date Range: 1/1950 - 10/2009.).

Table 3: Cross-correlations between the monthly central England surface temperature IMFs and climate factor IMFs

	AMM	AMO	AO	JMA	NAO	PDO	QBO	SUN
Original	−0.0175	0.1188	0.2069	0.0708	0.07	0.0432	−0.0782	−0.0205
Mode 1	−0.0091	0.0098	0.2988	0.0455	0.195	0.0291	−0.0855	−0.0532
Mode 2	−0.1037	0.1928	0.0995	0.1616	0.0197	0.1499	−0.2335	−0.0115
Mode 3	0.0854	0.2473	−0.0135	0.0384	−0.0945	−0.1381	0.2731	0.0847
Mode 4	0.0347	0.2137	0.0352	0.0058	0.007	−0.1358	0.1365	−0.0565
Mode 5	0.0857	0.1792	0.3639	0.1972	0.101	−0.0053	−0.0786	0.2364
Mode 6	−0.5748	−0.4658	0.2871	−0.5123	0.1796	−0.3476	0.0824	0.213
Mode 7	−0.2625	0.2612	0.0688	−0.776	−0.2609	−0.6932	−0.5404	0.0342
Mode 8	−0.0484	−0.1692	0.7405	0.744	0.625	0.4741	−0.441	−0.7316
Trend	0.4784	0.9997	0.3506	0.9995	−0.9202	0.7293	0.6906	−0.7151

If $|r| \geq 0.074$ correlation is considered to be statistically significant ($p < 0.05$, color = red); If $|r| \geq 0.130$ correlation is considered to be extremely statistically significant ($p < 0.001$, color = pink); Number of Samples: N = 718 (Date Range: 1/1950 - 10/2009).

In Figures 10a and 10b we present the significance levels of the cross-correlations in Tables 2 and 3. In Table 2 and the Left Panel of Figure 9, the long-term trends of the GSTA and the above listed climate factors are highly statistically, correlated. Those correlations with the AMO, JMA and NAO are nearly identical, though the correlation with the NAO is negative. There are also high correlations between the GSTA trend and the AMM, AO, PDO, QBO and the SUN, though those with the NAO and SUN are negative. The original time series of the AO, JMA and AMO time series are significantly correlated with the GSTA. Modes 3 through 8 of the GSTA and the AMM and AMO are significantly correlated. The GSTA is significantly corre- lated with: Modes 2-8 of the ENSO/JMA; Modes 3–8 of the AMM; Modes 1 - 5 and 7-8 of the AO; Modes 5, 7 and 8 of the NAO; Modes 5-8 of the PDO; Modes 5 and 8 of the QBO; and Modes 5, 6 and 8 of the SUN, with 8 negatively correlated.
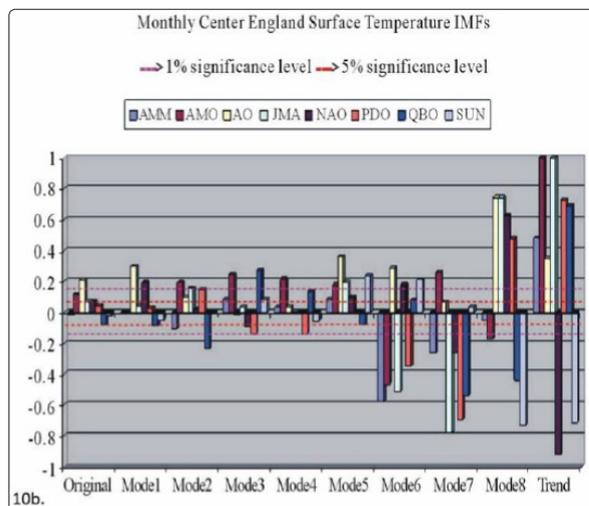

10a.

10b.

Figure 10: Blocks of the "r" values of the Cross-Correlations between: a. GSTA time series IMFs; b. Central England Surface Temperature time series IMFs. Both (a) and (b) versus selected Climate Factor IMFs. The 1% and 5% significance levels are indicated. If $|r| \geq 0.074$ correlation is considered to be statistically significant ($p < 0.05$, color = red); If $|r| \geq 0.130$ correlation is considered to be extremely statistically significant ($p < 0.001$, color = pink); Number of Samples: N = 718 (Date Range: 1/1950 - 10/2009).
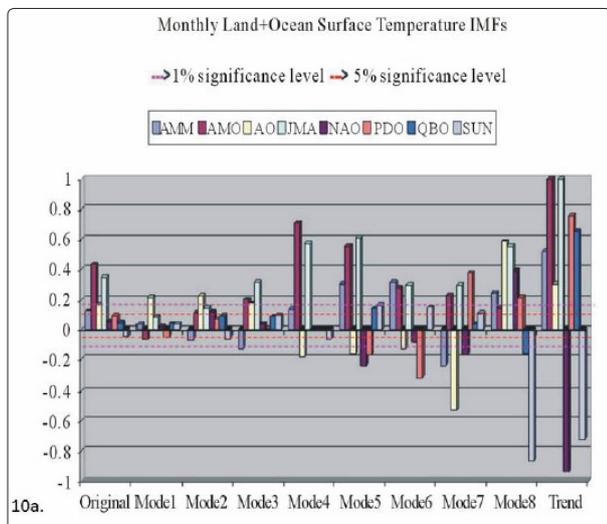
In Table 3 and the Right Panel of Figure 10, and identical to that of the GSTA, the long-term trends of the CE and the above listed climate factors are highly statistically, correlated. Those correlations with the AMO, JMA and NAO are almost identical, though the correlation with the NAO is negative. There are also high correlations between the CE trend and the AMM, AO, PDO, QBO and the Solar Cycle, though those with the NAO and Sun are negative. The original time series of the CE time series is only significantly correlated with the AO. The CE IMF modes are significantly correlated with: Modes 5 and 6 of the AMM; Modes 2 - 8 of the AMO, with Modes 6 and 8 negatively; Modes 2 and 5 - 8, of the ENSO modes, with 6 and 7 being negative; Modes 1, 5, 6 and 8 of the AO; Modes 1 and 6 - 8 of the NAO, with 7 negative; Modes 2 - 4 and 6- 8 of the PDO, with 3, 4, 6 and

7 negative; Modes 2, 3, 4 and 7, 8 of the QBO, with 2, 7 and 8 negative; and Modes 5, 6 and 8 of the Sun, with Mode 8 negative. In Figures 11a, b, we present the time series and EEMD decompositions of water levels at Sewell's Point VA and Atlantic City NJ. Curiously, the VA coastal time series displays 8 IMFs while the NJ IMFs show 9. The NJ time series is 5 years longer than that of VA and displays a nearly record length mode; which cannot show up in the VA time series for lack of length of time. Here, several authors have claimed that Gulf Stream Current (GSC) lateral meanders could directly contribute to coastal sea levels along the eastern seaboard. Several studies contend that there was an influence of the Gulf Stream on coastal sea level at Charleston SC and at Sewell's Point VA, respectively, but Atlantic City is not mentioned in those studies [26,27]. In the grand scheme of effecting variability in coastal sea level, the GSC is 150 km offshore of Charleston, and since the e-folding width influence of the GSC only extends about 20 kilometers coastward it cannot dynamically affect water levels at Charleston [28]. This would seem to demonstrate a lack of correlation between the GSC's shelf position and coastal sea level; save for Cape Hatteras per se which is within 20 km of the GSC there. The Sweet et al study did not consider an especially wet spring in the coastal domain of SC in the period of the study, June-July 2009, which is believed (National Weather Service Forecast Office, Charleston, p.c.) to have accounted for the rise in sea level in Charleston; which is at the confluence of three rivers [26]. Likewise, while the Ezer et al study presents a case for GSC induced variability in water level variability in the Chesapeake Bay system, in the publication, there is a focus on the water level record from Baltimore MD, which is some 300 km upstream from the mouth of the Bay [27]. That water level record is more likely affected by local precipitation and river watershed flow variabilities, and then from the GSC, which is ~ O (400 km) away from Baltimore.

To determine if the GSC, could have an influence on coastal sea level along the U.S. Atlantic Eastern Seaboard, we consider a 3-monthly time series of GSC transport through the Florida Straits. We present the EEMD IMFs of the 30-year GSC time series in Figure 12a along with a contemporaneous North Atlantic Ocean Basin Heat Content plot down to 700m, Figure 12b. In Figure 12a we find that the 40 year time series of the GSC reveals a rich 25-40 Sverdrup (1 Sverdrup = 10^6m^3/s) transport. IMF mode C1 is 3 months, C2 is 6 months, C3 is 1 year and C4 is 2-4 years. C5 is 11 years from 1982-1994 and then from 1995 to 2012 transitions to 5-7 years. C6 is 15 years and C7 is 22 years. C8, the trend appears to be relatively flat but could actually be the first half of a 60-70 year cycle. In Figure 12b we see that the 55-year, 3-monthly averaged time series of North Atlantic Ocean Basin Heat Content time series displays IMFs of 6-monthly, annual, 2-4, 11, 22 and 33 years. Here we have evidence that Heat Content may be the source of the enigmatic 22 and 33-year signals that manifest themselves variously in the Coastal Sea Level records alluded to in Figures 2, 10 and 11. The trend is ~ of 1.5 (10^{23}) Joules, a significant rise over the 55-year heat content record. It is of note here that the Pacific Ocean Basin Heat Content map (not shown) also reveals 22 and 33-year signals. Moreover, the 30- year record that we have presented does not indicate any record-length- trend increase or decrease in transport; and thus no contribution to long-term sea level variability or trends unless the slight bubble in the trend is actually the first half of a 60-70 year cycle.
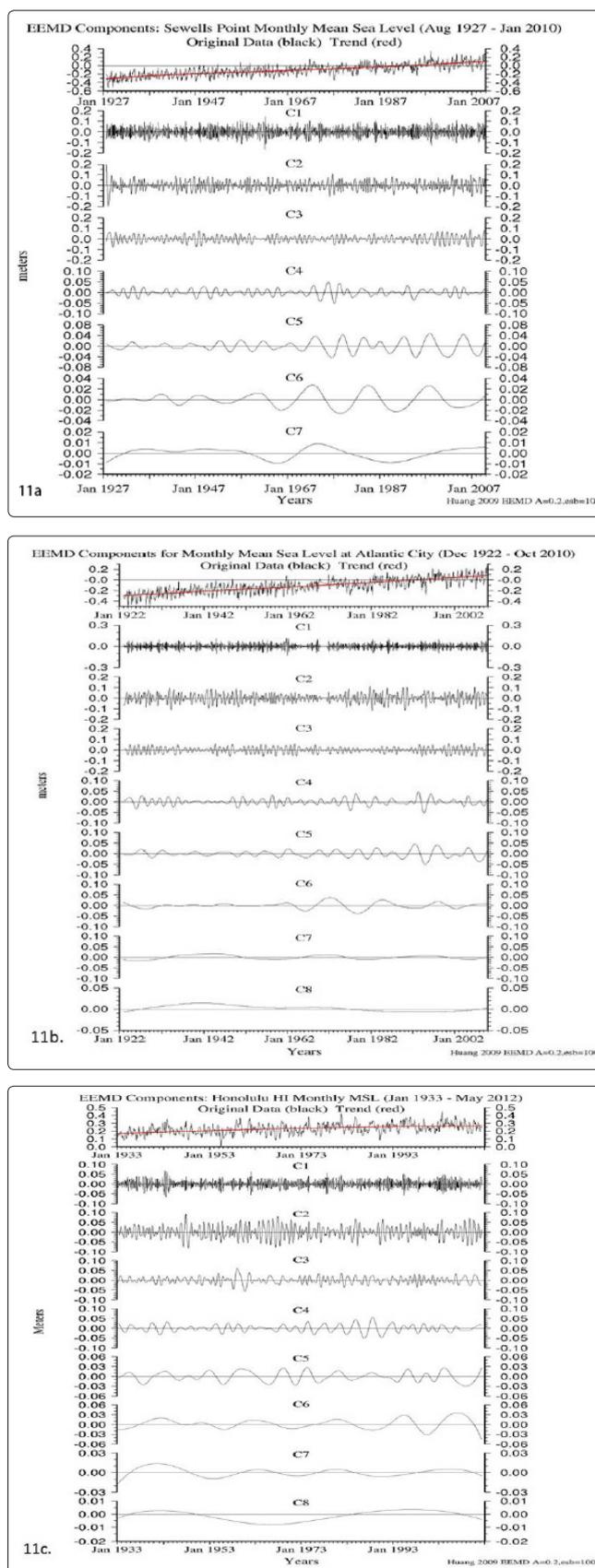

Figure 11: EEMD IMS of coastal water level time series at: a. Sewell's Point VA; b. Atlantic City NJ
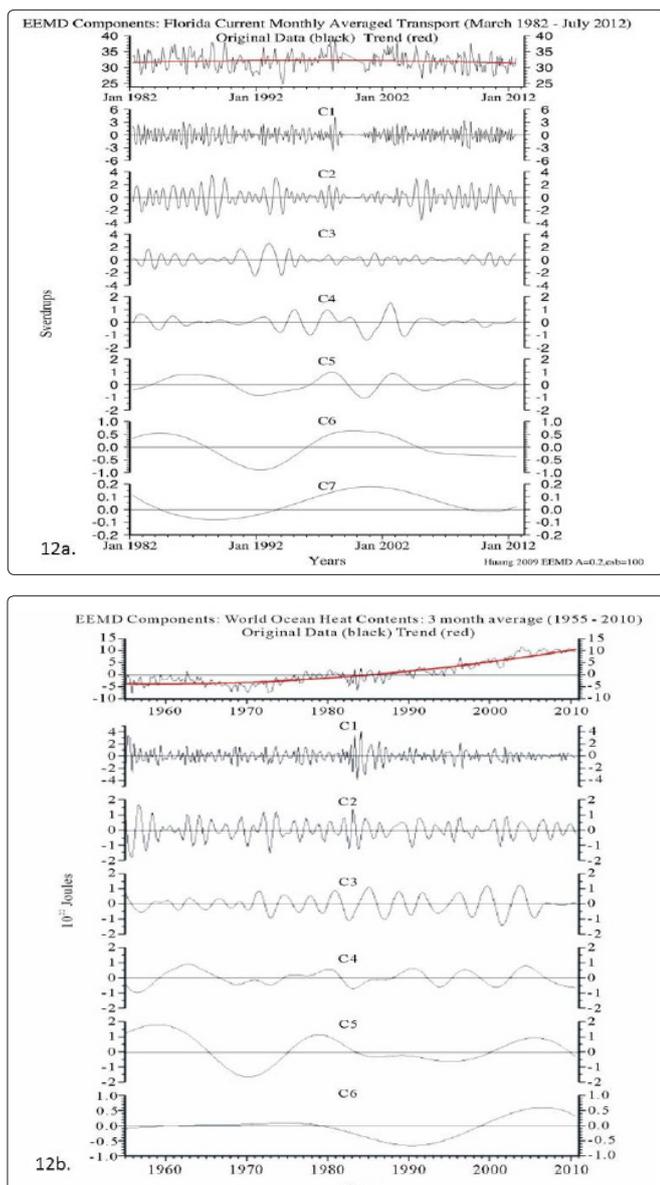
Figure 12: EEMD IMFs of: a. GSC monthly time series collected in the Florida Straits; b. the North Atlantic Ocean Basin Heat Content down to 700 m.

From a climate perspective, the increased heat content and the warming of the surface waters of the North Atlantic and Pacific Oceans suggests that the Atlantic Meridional Ocean Circulation (AMOC) should have slowed down, thus calling for an acceleration in GSC, but no such response is evident in the GSC time series. The closeness of the Gulf Stream to Cape Hatteras NC suggests that coastal sea level at the site could be affected by Gulf Stream lateral motions. However, Pietrafesa et al found no such relationship in a large field program conducted in the Cape Hatteras Confluence. Lateral swings in the Gulf Stream downstream (to the north) of Cape Hatteras from a more westward shelf-break hugging mode to an offshore mode were discussed in Bohm et al but there again, no effect of the Stream lateral locale on coastal water levels downstream of Cape Hatteras was evident.

Figures 13 a, b present a composite of representative temperature and coastal water level trends. The water level trends are normalized to zero for representative comparisons. Table 2 summarizes the trends. Throughout the U.S. there are great variations in air temperature and coastal water level trends from city to city in the U.S. For example, Grand Rapids SD and Fairbanks AK air temperatures have increased at more than double the U.S rate and four times the GSTA, while those of Asheville NC, at the peak of the mid-latitude Appalachian Mountains and Honolulu HA, in the middle of the Tropical Pacific Ocean, are at the global rate of warming. Again, these trend calculations are not possible, other than be employing HHT and EEMD. Sea level rates of rise are clearly very variable as a function of locale, around the U.S. coastlines of the Eastern Seaboard, the Gulf of Mexico, the Pacific Coast, including Alaska and Hawaii and Holland. Sewell's Point VA, Atlantic City NJ and Galveston TX are relative "hot spots". There is a strong grouping of stations including Pensacola FL, Charleston SC, San Diego CA, San Francisco CA, Boston MA and Delfzig Holland (the Netherlands), and then with lower rates of rise in Honolulu, HA and the South China Sea. The differing rates of sea level rise have much to do with regional to local scenarios, such as groundwater removal, river sediment loading, year-to-year variations in seasonal steric adjustments, increases and decreases in precipitation and subsequent river discharges, and so on. What is clear is that, as shown by the GOSTA rate of warming, the Global Ocean is the regulator or thermostat of the planetary global surface temperatures; comparing the GLSTA to the GOSTA to the GSTA as presented in Table 3.
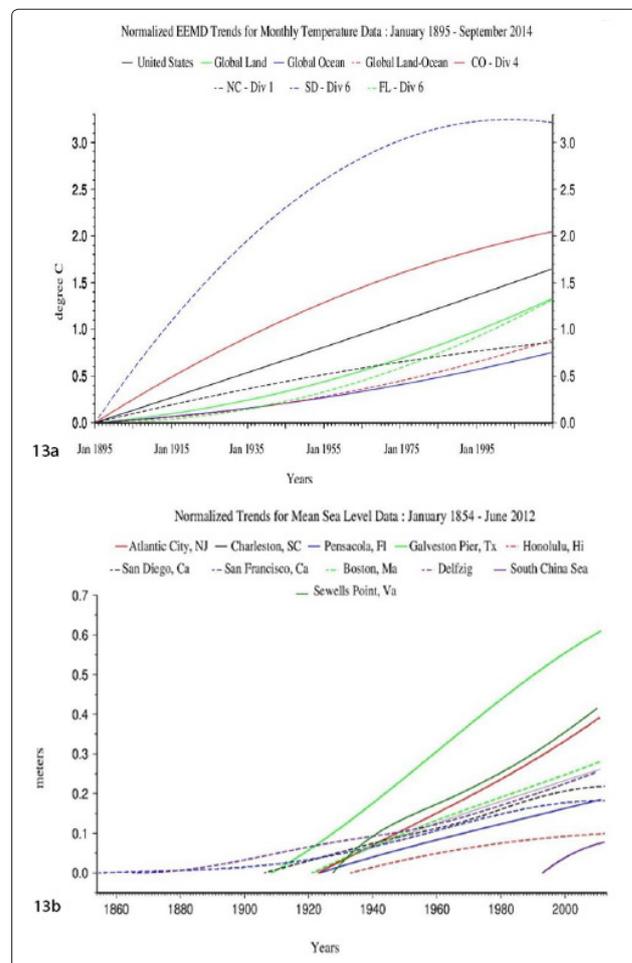

Figure 13: a. Temperature trends for the Global Ocean, the Global Land- Atmosphere, the Global Ocean + Land-Atmosphere, Boulder-Colorado, Asheville –North Carolina, Sioux City–South Dakota, Miami-Florida, the Continental States of the U.S.A. multiple in-situ station locations; b. Coastal water level trends for multiple in-situ station locations.

In Table 4 we display record length trends, respectively for record length global air and ocean surface temperatures and for specific representative cities in the U.S. and for coastal sea levels. It is of note here that by employing HHT and EEMD we are able to compute record length trends, which are distinct from the end-points of the various time series. The end-points contain all of the onset and final values of the nonlinear time series and are revealed in the decomposition. This is a great virtue of HHT and EEMD.

Table 4: Trends of Selected Temperatures and Selected Sea Levels

Temperatures (T)	°C/Decade	Sea Level (SL)	mm/Decade
Global Ocean Temperature	0.058	Atlantic City NJ	0.459
Global Land	0.102	Boston MA	0.300
Global Ocean + Land	0.067	Charleston SC	0.280
Continental US	0.138	China Sea	0.432
Asheville NC	0.072	Delfzig Holland	0.261
Boulder CO	0.171	Galveston TX	0.612
Grand Rapids SD	0.269	Honolulu HA	0.140
Miami FL	0.110	Pensacola FL	0.210
Fairbanks AK	0.279	San Diego CA	0.204
Honolulu HA	0.081	San Francisco CA	0.174

We next look at several revealing plots in keeping with the cross-correlation analyses and the EEMD IMF decompositions revealed previously in the text; therein comparing several climate factors to each other and to state variables. We shall pursue that approach and consider a series of global to regional time series of atmospheric and oceanic temperatures, coastal water level data, and wind data. We again note that precipitation data are available for relatively long time series but are dominated by zeros and are thus difficult to work with mathematically unless monthly data are used, and that compromises the high frequency portion of the spectrum. We first compare the yearly averages of the AO to the NAO and PDO to ENSO, all shown to be of importance in global temperatures. The AO and NAO, Figure 14a, overlay in amplitude and are phased-locked. ENSO and the PDO, both Pacific Ocean Basin phenomena, Figure 14b are quite similar, but not identical in amplitude and phase.
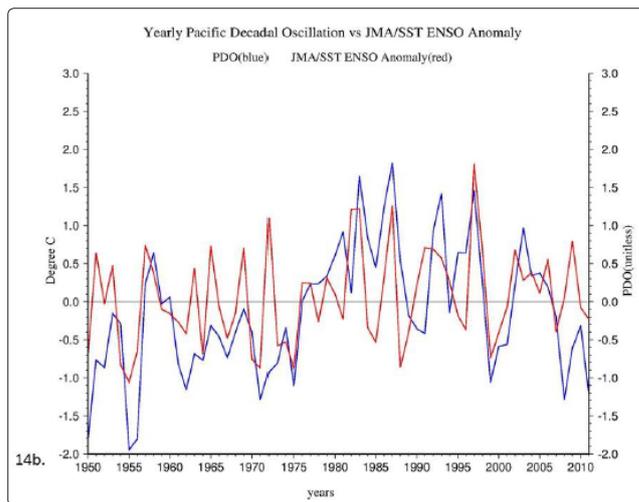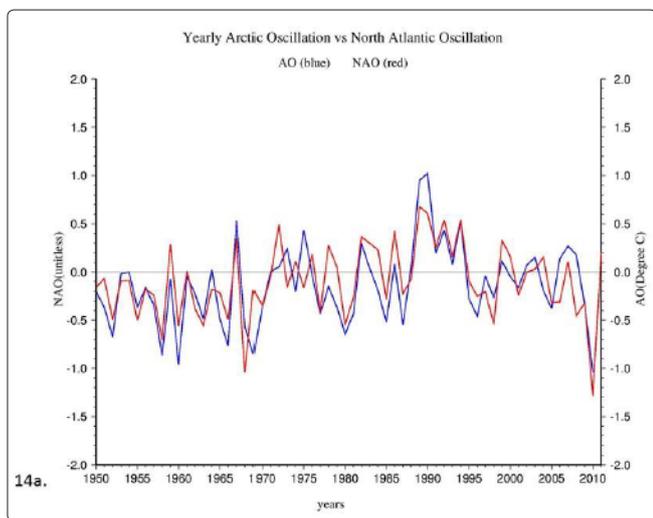

14a.

14b.

Figure 14: Annual averages of: a. AO vs. the NAO; b PDO vs. ENSO.

The AO (or Northern Annular Mode/Northern Hemisphere Annular Mode, NAM) and NAO are indices which vary over time with no particular periodicity of the dominant pattern of non-seasonal sea-level pressure variations north of 20°N latitude provided in the literature [25]. The authors find that the AO is supposedly characterized by pressure anomalies of one sign in the Arctic with the opposite anomalies centered about 37°–45°N. However, we find that positive and negative phases of the AO and the NAO more likely determine the degree to which Arctic air penetrates into middle latitudes and are defined by surface atmospheric pressure patterns and that there are very distinct intrinsic well-defined modes of variability buried within the data set. The AO and NAO are zonally and meridional symmetric and sea-saw's between sea level pressures in polar and temperate latitudes. When the AO index is positive, surface pressure is low in the polar region. This enhances the middle latitude Jet Stream to blow strongly and consistently from west to east, thus keeping cold Arctic air locked in at higher latitudes. When the AO index is negative, there is high pressure in the polar region, weaker zonal winds, and greater movement of frigid polar air into the middle latitudes. In Figure 16b we see that there appear to have been several climate factor shifts in both records in the mid-1970s and then again at the turn of the century from the 20th to the 21st. These Pacific Ocean Basin wide shifts could have resulted in significant wind stress patterns across the Pacific in addition to steric rises and falls along and across the Pacific. We will test this observation. Consider Figure 15a, b in a plot of annually averaged sea level at San Francisco vs. ENSO and the PDO.
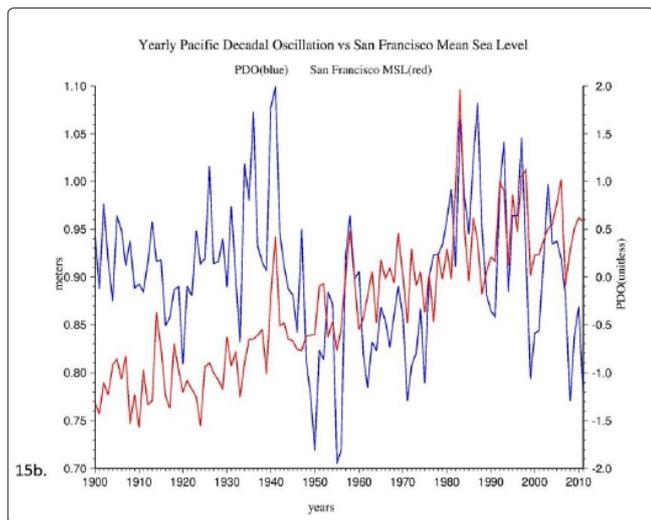

15a.
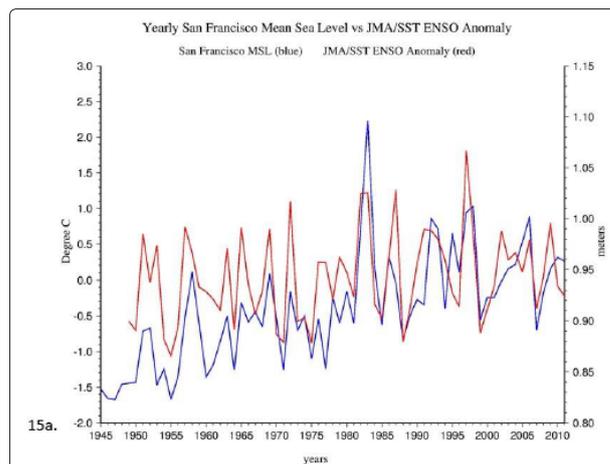
Figure 15: Annual averaged San Francisco sea level vs.: a. the ENSO; b. the PDO

Figure 15 suggests that sea level along the west coast of the U.S. (east coast of the Pacific Ocean Basin) can be enhanced or suppressed by the order of 10 to 20 centimeters from year to year, in association with wind fields changing in keeping with ENSO and the PDO. Obviously, these pattern shifts also must have resulted in Pacific Ocean Basin wide adjustments to its thermohaline field and its thermocline. The apparent trends of both the PDO and ENSO to colder (warmer) phases foreshadow relative overall drops (rises) in eastern Pacific coast sea level and rises (drops) in western Pacific coast sea level. The Pacific" Latitudinal Sea Level Sea Saw" is functioning. Nevertheless, all other climate factors must be considered.
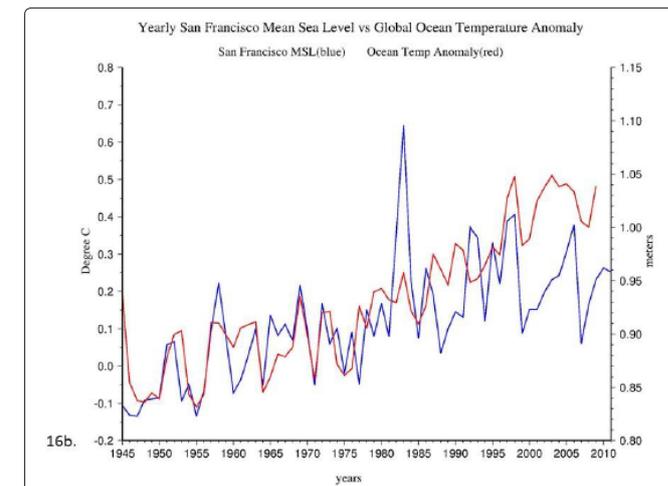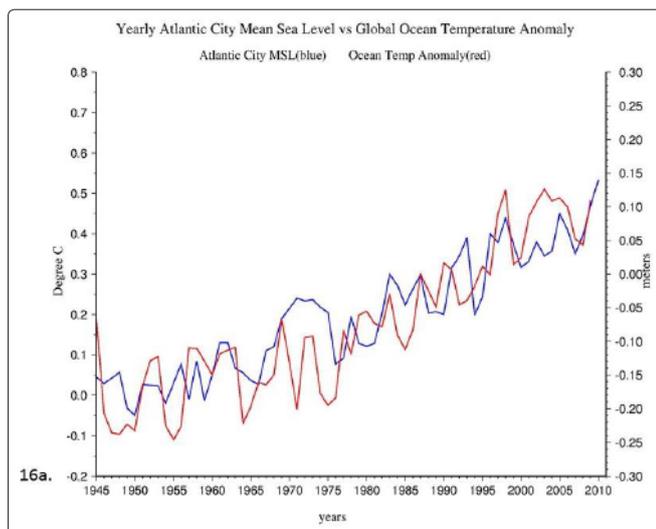
Figure 16: Yearly Sea Levels vs the Global Ocean Temperatures: a. Atlantic City vs. GOSTA; b. San Francisco vs. GOSTA

We recall that in Table 2, that if the "r" factor was such that |r | ≥ 0.130, then the correlation was considered to be "extremely statistically significant". Further, the GSTA (GLSTA and GOSTA by association) IMFs vs. the AO IMFs were all high, ranging from 0.13 to 0.59. Therefore, we now use the GOSTA as a surrogate and compare the annually averaged water levels at Atlantic City NJ to the GOSTA. If temperatures are relatively high in the North Atlantic Ocean Basin then water levels are also relatively high along the coastlines (Figure 16a). The same is true in the Pacific Ocean Basin (Figure 16b). However, we next drill down further to see if in addition to the steric rises and falls of the Atlantic and Pacific Ocean Basins, if there are manifestations of daily to monthly to seasonal to yearly to decadal to multi-decadal water level variability as a function of coastal alongshore winds. This would be in keeping with the findings of Chao and Pietrafesa and Pietrafesa et al [28].

In Figures 17a and 17b, we see that the EEMD IMFs of sea level and alongshore winds at Charleston have virtually identical decompositions, excepting for the trends (red lines in the top panels), over the time scales of the 60 year record shown. In Figure 17c we see that the correlation of sea level vs. alongshore winds is highly inversely correlated over all time scales over a 65 year period. They are in harmony with sea level rises and falls following the wind. The winds do not show record length increases or decrease while sea level does; provided in Table 3. On the daily time scale, as shown in Figure 18a, daily averaged alongshore winds drive daily averaged water levels; with the caveat of an 8-hour lag as first reported by Chao and Pietrafesa [28]. If the winds blow with the coast to the left (right) coastal sea level will fall (rise). This is in keeping with the wind-sea level correlation in Figure 17c.
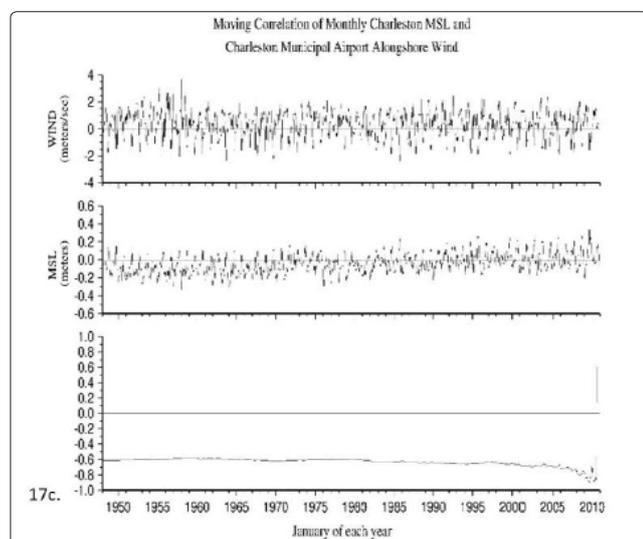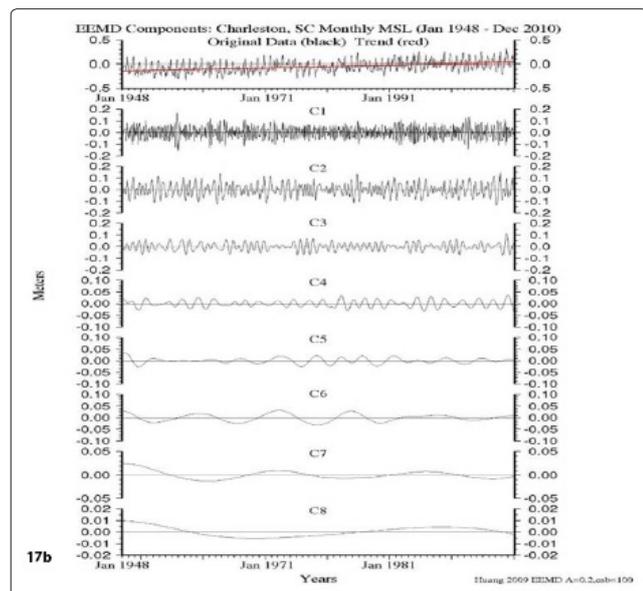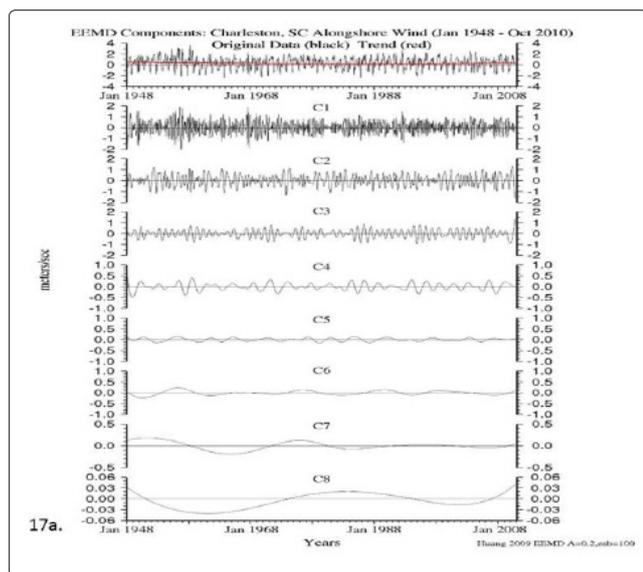
Figure 17: a. EEMD IMFs of monthly Alongshore Coastal Winds at Charleston; b. EEMD IMFs of Water Level at Charleston; c. Moving Correlation of Water Level time series vs. Alongshore Coastal Wind time series shown in the uppermost lines of (a) and (b).

In the daily to climate scale spectrum of sea level variability, in Figure 18b we find that coastal sea levels along the northeastern seaboard of the U.S. and that of Holland align with the rise in heat in the North Atlantic Ocean Basin over climate scales. The water levels along both sides of the meridional boundaries have moved upward in concert with the rise of the North Atlantic Ocean.
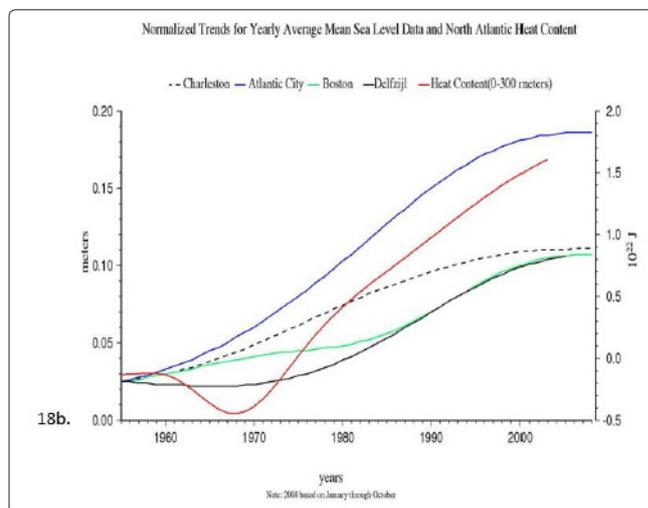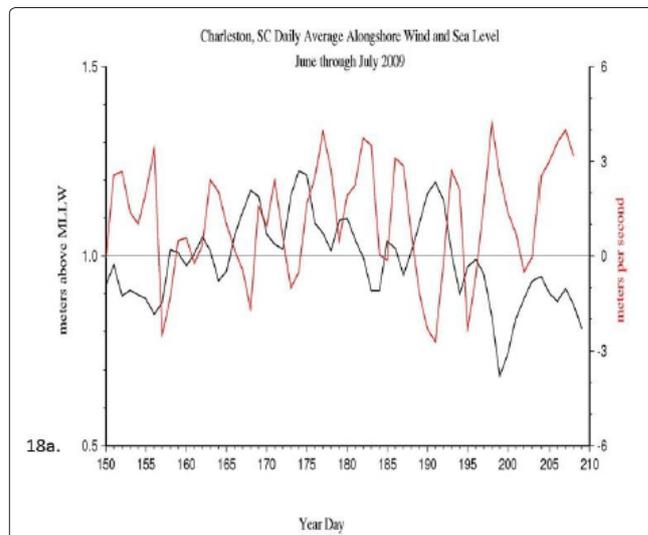

Figure 18: a. Daily Alongshore Winds and Water Levels at Charleston; b. Sea Level Trends at selected U.S. and Holland stations vs. North Atlantic Ocean Basin Heat Content (down to 300 meters).

Conclusions
We have harvested and interrogated a multitude of atmospheric and oceanic state variables and Solar - Earth system lengthy time series. Using an intrinsic mode decomposition methodology, the HHT-EEMD, we revealed internal modes of temporal and spatial amplitude and frequency - modulated variability signals across the ranges of higher frequency "weather" to lower frequency "seasonal" to "sub-seasonal" to very low frequency "climate" scales. The modes document the existence of an Earth planetary weather to climate sequence common across the families of atmospheric and oceanic temperatures, atmospheric pressure, and coastal water levels, in-kind. "weather" ranges from minutes to hours to days to weeks, as shown in Table 1. Also shown in Table 1, seasonal variability ranges from two, three and six months. Sub-seasonal extends from annual to inter-annual, 2-4, 4-7 and 5-7 years. Lower frequency, climate variability signals are 11, 22 and 33 years. Longer period climate signals are 65-70 and

120-140 years. The Global Ocean, with the enormous capacity of seawater to absorb and retain heat has acted as the planet's throttle and modulator. However, the Oceanic Heat Content has been driven upward by the fact that 19 of the warmest years on record have occurred in the past 20 years. The atmosphere is the planetary delivery system.

Our findings regarding the Earth's weather to climate system are instructive in the construction of the atmospheric and an oceanic phenomenology temporal Table 1; which provides definition to the spectrum of weather to seasonal to sub-seasonal to multi-year at decadal to multi-decadal to centennial variability in the Earth's atmosphere and ocean. The Thermohaline Circulation or Global/ Great Ocean Conveyor Belt is the lower low frequency oceanic redistribution system, related to Solar activity at that period.

Thus, we show that atmospheric and oceanic variability are the result of a suite of nonlinear and non-stationary phenomena that are individually identifiable and are occurring simultaneously and inter-actively. We propose that the weather to climate spectra in both the atmosphere and the ocean, actually constitute an over-lapping continuum, with shorter period oscillations riding atop longer period oscillations and then atop overall record length trends; that is that they are multi-scale. Therefore, we propose that for the atmosphere and the ocean, the terms weather, seasonal and sub-seasonal variability, and climate variability, are all distinctly separate harmonics, with well-defined frequency and amplitude modulated banded peaks across a spectrum of multi-scaled phenomena. Weather resides at the high frequency end of the spectrum and climate is at the low frequency end of the spectrum. Seasonal and sub-seasonal variability are everything in between. The phenomena are distinct but interactively coupled and collectively they run the gamut from what we commonly refer to as weather to climate riding atop record length trends. In final summary we point out that we have addressed and answered Bothe's question of "when does weather become climate". Our answer is that weather and climate are distinct in the overall continuum of weather to climate [29-38].

Author Contributions
L.J. Pietrafesa conceived of the research concept to couple data derived from in-situ and satellite data to decompose a variety of oceanic and time series to investigate weather, seasonal, sub-seasonal and climate variability and climate scale trends' and definitions therein. He also curated some of the data and interpreted the results. Bao also curated the data and contributed to the interpretations of the data and production of the figures. Gayes contributed to data interpretation and provided research study support.

References
1. Cheng Qian, Congbin Fu, Zhaohua Wu (2011) Changes in the amplitude of the temperature annual cycle in China and their implication for climate change research. Journal of Climate 24: 5292-5302.
2. Franzke C (2012) Nonlinear trends, long-range dependence, and climate noise properties of surface temperature. Journal of Climate 25: 4172-4183.
3. Ji F, Z Wu, Huang J, EP Chassignet, 2014. Evolution of land surface air temperature trend. Nature Climate Change 4: 462:466.
4. Geer I (1996) Glossary of Weather and Climate and related Oceanic and Hydrology Terms. American Meteorological Society Press 272.
5. Geer I (2000) Glossary of Weather and Climate and related Oceanic and Hydrology Terms. American Meteorological Society Press. 2nd Edition 272.
6. Bendat JS, AG Piersol (1986) Random Data, Analysis and Measurement Procedures, 2nd ed., New York: John Wiley and Sons 566.
7. Pattulo J, W Munk, R Revelle, E Strong (1955) The Seasonal Oscillation in Sea Level. Journal of Marine Res 14: 88-155.
8. Pietrafesa LJ (1976) Sea Level Variability on the North Carolina Coast. Center for Marine and Coastal Studies 6:110.
9. Loder JW, C Garrett (1978) The 18.6 Year Cycle of Sea Surface Temperature in Shallow Seas due to Variations in Tidal Mixing. Journal of Geophysical Research, Oceans 83: 1967-1970.
10. McKinnell, S.M. and W.R. Crawford, 2007. The 18.6 Year Lunar Nodal Cycle and Surface Temperature Variability in the Norteast Pacific Ocean. Journal of Geophysical Research, Oceans. 111:15.
11. Orlanski I (1975) A rational subdivision of scales for atmospheric process. Bull. Am. Meteorol. Soc 56: 527-530.
12. Hill MN (1960) The Sea. Ideas and Observations on Progress in the Study of the Seas. 809 Vol. 1: Physical Oceanography. 864 pp. Wiley Press.
13. Rahmstorf S (2003) Thermohaline circulation: The current climate. Nature 421: 692-699.
14. James and James (1976) The Mathematical Dictionary. 4th Edition. D. Van Nostrand Com. Pub.
15. Chatfield C (1975) Statistics for Technology. Chapman and Hall Pub 384.
16. Granger CWJ (1966) The typical spectral shape of an economic variable. Econometrica 34 : 150-161
17. Silver N (2012) The Signal and the Noise. Penguin Press.
18. Wu Z, NE Huang, JM Wallace, BV Smoliak, X Chen (2007) On the time-varying trend in global-mean surface temperature. Climate Dynamics 37: 759.
19. Wu Z, NE Huang (2009) Ensemble Empirical Mode Decomposition: a noise-assisted data analysis method. Advances in Adaptive Data Analysis 1: 1-41.
20. Huang NE, Z Shen, SR Long, MC Wu, EH Shih, et al. (1998) The empirical mode decomposition and the Hilbert spectrum for nonlinear and non-stationary time series analysis. Proc. Roy. Soc. Lond 454: 903-993.
21. Gabor D (1946) Theory of communication J IEE 93: 429-457.
22. Van der Pol B (1946) The fundamental principles of frequency modulation, Proc. IEE 93: 153-158.
23. Flandrin P, G Rilling, P Gonçalves (2004) Empirical mode decomposition as a filter-bank. IEEE Signal Proc Lett 11: 112-114.
24. Both O (2019) When does weather become climate? EOS, August 14, 2019.

25. Cohen J, M Barlow (2005) The NAO, AO and Global Warming: How closely related?, Journal of Climate V 18: 4498-4513.
26. Sweet W, C Zervas, S Gill (2009) Elevated East Coast Sea Level Anomaly: June-July 2009. NOAA Technical Report. NOS CO-OPS 51: 40.
27. Ezer T, LP Atkinson, WB Corlett, JL Blanco (2013) Gulf Stream induced sea level rise and variability along the US mid-Atlantic coast. Journal of Geophysical Research: Oceans 118: 685-697.
28. Chao SY, LJ Pietrafesa (1980) The sub-tidal response of sea level to atmospheric forcing in the Carolina Capes. Journal of Physical Oceanography 10: 1246-1255.
29. Huang NE, Z Shen, SR Long (1999) A New View of Nonlinear Water Waves– The Hilbert Spectrum, Ann. Rev. Fluid Mech 31: 417-457.
30. Huang NE, ML Wu, SR Long, SS Shen, WD Qu, et al. (2003) A confidence limit for the Empirical Mode Decomposition and Hilbert Spectral Analysis. Proc. Roy. Soc. London 459: 2317-2345.
31. Huang NE, Z Wu (2008) A review on Hilbert-Huang Transform: the method and its applications on geophysical studies. Rev. Geophys 46: RG2006
32. Huang NE, Z Wu, SR Long, KC Arnold, X Chen, et al. (2009) On instantaneous frequency, Advances in Adaptive Data Analysis 1: 177-229.
33. Ljung, GM, G E P Box (1978) On a Measure of Lack of Fit in Time Series Models. Biometrika 65: 297-303.
34. Sabra K, B Cornuelle, W Kuperman (2016) The Rising Heat Content of the Earth's Oceans. Physics Today 32.
35. Shakespeare W (1603) Hamlet, Quarto Ed: https://www.britannica.com/topic/Hamlet-850 by-Shakespeare.
36. Stanley T (1687) Pythagoras: His Life and Times. 2010. Re-Issue, On-line as Pythagoras: his life and Teaching. Ibis Press.
37. Wu Z, NE Huang (2004) A study of the characteristics of white noise using the empirical mode decomposition method, Proc. Roy. Soc. London 460: 1597-1611.
38. Wu Z, Huang NE, Long SR, Peng CK (2007) On the trend, detrending, and variability of nonlinear and nonstationary time series. Proceedings of the National Academy of Sciences 104: 14889-14894.